

# Comparison of the ageing behaviour of PM 2124 Al alloy and Al–SiC<sub>p</sub> metal-matrix composite

M. P. THOMAS, J. E. KING

*Department of Materials Science and Metallurgy, University of Cambridge, Pembroke Street, Cambridge CB2 3QZ, UK*

The ageing response of 2124 Al–SiC particulate metal-matrix composite (MMC) and unreinforced alloy has been examined using hardness measurements and Arrhenius analysis. The formation of phases during precipitation has been studied using differential scanning calorimetry (DSC). The MMC exhibits accelerated ageing compared to unreinforced alloy, due to enhanced S' formation. The activation energy for diffusion is lower in the MMC than in the unreinforced alloy. DSC scans show Guinier–Preston B (GPB) zone nucleation to occur at a lower temperature in the MMC, whilst the total volume of GPB zones formed is smaller than in the unreinforced alloy. A model has been proposed to explain the GPB zone formation behaviour, in which ease of GPB zone nucleation varies within the MMC, as a function of ageing time and of position within the matrix. S' formation is enhanced in the MMC because of improved diffusion and a large increase in density of heterogeneous nucleation sites compared to the unreinforced alloy.

## 1. Introduction

One of the main factors limiting the use of Al metal-matrix composites (MMCs) for engineering components is a lack of property characterization in relation to unreinforced Al alloys. This lack of data extends from processing parameters to final mechanical properties. During ageing, for example, many MMCs appear to reach peak hardness faster than the corresponding unreinforced Al alloy [1–11]. Most studies to date, however, draw conclusions about the ageing behaviour of Al MMCs from only one or two ageing temperatures [1–9, 12, 13]. It is more useful to examine the ageing response of the MMC over a wide range of temperatures and compare this directly with the unreinforced Al alloy [10, 11, 14]. The present study combines detailed hardness measurements, Arrhenius analysis and differential scanning calorimetry (DSC) to examine the differences in ageing between a particulate-reinforced MMC and the unreinforced matrix alloy, over a range of ageing temperatures.

## 2. Experimental procedure

### 2.1. Material

The material is a 2124 (Al–Cu–Mg) alloy containing 20 wt % (17.9 vol %) of SiC particles (SiC<sub>p</sub>), with a nominal particle size of 3–5 μm. The MMC was produced via powder blending, canning, degassing and hot isostatic pressing, followed by extrusion to plate of 75 mm × 18 mm cross-section. The extrudate was solution-treated at 505 °C for 2 h and given a 1.5% permanent stretch. It had been naturally aged

for one year prior to this study. Unreinforced 2124 Al alloy was manufactured via the same production route, although it was not stretched. All materials were supplied by BP Metal Composites, Farnborough, UK.

The MMC was studied in two conditions: as received (stretched and naturally aged) and re-solution treated (505 °C for 2 h and cold-water quenched). The unreinforced alloy was subjected to the same solution treatment prior to examination.

Figs 1 and 2 show the microstructure of the two materials. It is clear that solution treatment has not resulted in recrystallization. The grains in the unreinforced alloy are elongated in the L direction (and flattened in the T and S direction) producing a lath-like morphology (Fig. 1). The approximate range of grain sizes is 2–14 μm in the S and T directions and 8 to 60 μm in the L (extrusion) direction. Stringers of oxide and intermetallic particles were occasionally seen running in the L direction.

In the MMC, the SiC<sub>p</sub> are generally well distributed, although some matrix-rich areas are seen, elongated in the L direction (Fig. 2). Oxide and intermetallic stringers are also observed as in the unreinforced alloy. It proved difficult to etch the grain structure in the MMC clearly. Etching in Keller's reagent for a few seconds reveals the grain/sub-grain boundaries indistinctly, as can be seen in Fig. 2. Etching for longer periods exposes many sub-surface SiC<sub>p</sub> and obliterates the matrix grains. Grain/sub-grain growth in the MMC has obviously been limited by the presence of the SiC<sub>p</sub>, with most grains/sub-grains stretching be-

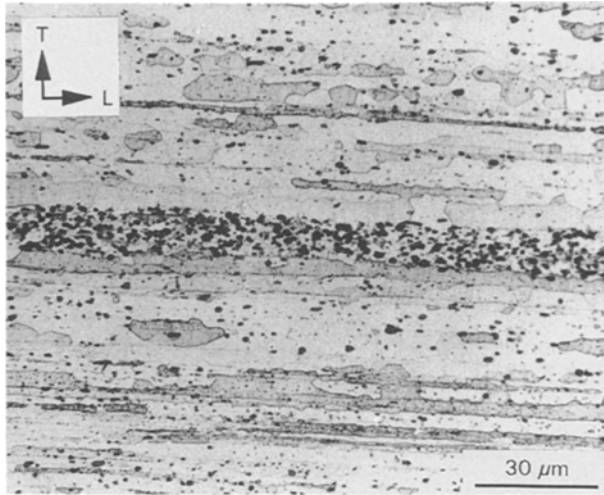


Figure 1 Optical micrograph of LT plane in the unreinforced Al alloy.

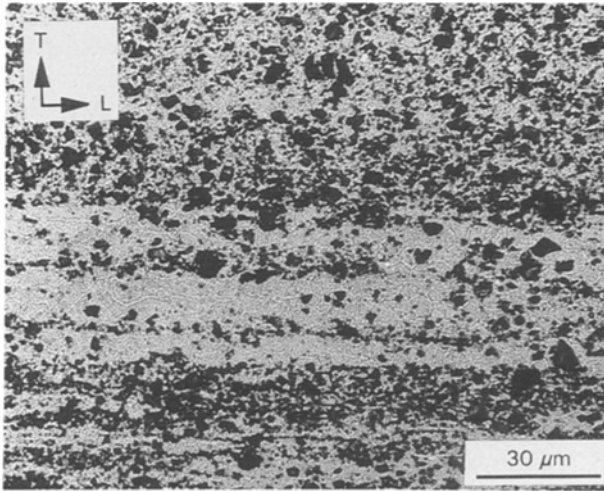


Figure 2 Optical micrograph of LT plane in the MMC.

tween neighbouring particles. The limiting effect of reinforcement on the grain growth of MMCs has been observed before [15, 16]. The approximate range of sub-grain sizes is 2 to 10  $\mu\text{m}$  in the T and L directions and 1 to 7  $\mu\text{m}$  in the S direction i.e. the grain/sub-grain structure is smaller in the MMC than in the unreinforced alloy.

## 2.2. Experiments

Ageing was carried out at a range of temperatures between 110 and 210  $^{\circ}\text{C}$  ( $\pm 3^{\circ}\text{C}$ ). Specimens had nominal dimensions of 10 mm  $\times$  10 mm  $\times$  5 mm. The ageing response of each material was monitored using Vickers macrohardness (10 kg load) measurements. Microhardness measurements on this MMC have been found to be too variable to be of use [17]. The hardness at each ageing interval was taken as the mean of five readings. Three ageing runs were conducted at each temperature for each material, making a total of 54 ageing curves.

Arrhenius analysis of MMCs is not often reported,

presumably due to the difficulty of obtaining reliable data. Both macro- and micro-hardness testing methods are open to criticism when used for Arrhenius analysis. Microhardness measurements, whilst being adequate to give an idea of the ageing behaviour of an MMC at a particular temperature, are probably too variable to produce accurate Arrhenius data at a wide range of ageing temperatures. Previous work by the current authors showed large fluctuations in the microhardness of the same MMC specimen at different points in the matrix [17]. This was attributed to the variable impingement of sub-surface  $\text{SiC}_p$ . For the present MMC this makes microhardness readings unsuitable for Arrhenius analysis. On the other hand it can be argued that macrohardness measurements, being a measure of the MMC hardness as a whole, should not be used in Arrhenius analysis which determines a property for the matrix alone.

A previous study involving Arrhenius analysis of MMC ageing used macrohardness measurements and the present authors have continued with this method [11]. The use of a 10 kg load ensures that the indentation is large enough not to be influenced by individual  $\text{SiC}_p$  particles, and an average hardness of the whole composite is measured. The hardness contribution of the  $\text{SiC}_p$  will shift the whole ageing curve to a higher hardness level. Since the  $\text{SiC}_p$  are not affected by the ageing process, however, their effect is constant and no shift in the ageing curve with time should be induced, other than that associated with the change in ageing response of the MMC matrix compared to the unreinforced alloy. Since Arrhenius analysis uses only the time to peak hardness and temperature of ageing, and does not use the absolute hardness values, the use of macrohardness measurements is still valid.

If it is assumed that (i) peak hardness corresponds to the same level of transformation in each case and (ii) ageing temperatures are low enough for the transformation to be diffusion controlled, then the activation energy for diffusion can be determined from the time to peak hardness. The Arrhenius equation for diffusion states that, for a given temperature [18]:

$$D = D_0 \exp\left(\frac{-Q}{RT}\right) \quad (1)$$

where  $D$  = diffusion coefficient,  $D_0$  = material constant,  $Q$  = activation energy for diffusion ( $\text{J mol}^{-1}$ ),  $R$  = universal gas constant ( $8.34 \text{ J deg}^{-1} \text{ mol}^{-1}$ ) and  $T$  = temperature (K). This can be written as:

$$\log D = \log D_0 - \frac{Q}{2.3R} \left(\frac{1}{T}\right) \quad (2)$$

$D$  may be replaced with  $1/t$  where  $t$  is the time to peak hardness, so that a plot of  $\log(1/t)$  against  $1/T$  for a range of temperatures should be linear with gradient  $-Q/2.3R$ , allowing the activation energy for diffusion,  $Q$ , to be calculated.

DSC tests were conducted on each material in the non-artificially aged condition, within 30 min of quenching where solution treatment had been applied. A Perkin Elmer DSC7 was used with a scanning rate of  $10^{\circ}\text{C min}^{-1}$ , a nitrogen purge gas and sample weights

of between 10 and 20 mg. Since the  $\text{SiC}_p$  play no part in the formation of the DSC curves, the effective mass of the MMC samples was taken as

$$(\text{Sample mass})_{\text{effective}} = (\text{Sample mass})_{\text{actual}} - \text{Mass of SiC particles} \quad (3)$$

The  $\text{SiC}_p$  content of the MMC is 20 wt %. Three separate scans were made for each material to test the reproducibility of results.

### 3. Results and discussion

#### 3.1. Hardness curves

Fig. 3 plots peak hardness against time to peak hardness for the materials. Data points in Fig. 3 are the mean of the three ageing curves generated at each temperature. The expected trend of increasing peak hardness and increasing time to peak hardness with decreasing ageing temperature is observed in all cases. The stretched MMC gives consistently higher hardness for a given ageing time than the re-solution treated MMC. This may be partly due to dislocation strengthening, but is thought to arise mainly from the more homogeneous and finer precipitate distribution resulting from stretching. Improvements in strength and hardness on ageing are commonly seen after stretching in both unreinforced alloys [19, 20] and MMCs [21].

The two MMCs exhibit accelerated ageing (i.e. shorter times to peak hardness) at all temperatures compared to the unreinforced alloy. This is shown more clearly by the conventional ageing curves of Fig. 4. Such accelerated ageing has been attributed to easier precipitate nucleation and growth because of the increased dislocation density in the MMC matrix [2, 3]. The dislocations are generated as a result of a mismatch of thermal expansion coefficients between the Al matrix and  $\text{SiC}_p$  [22]. The assumption of easier precipitate formation in MMCs will be examined in Sections 3.2 and 3.3.

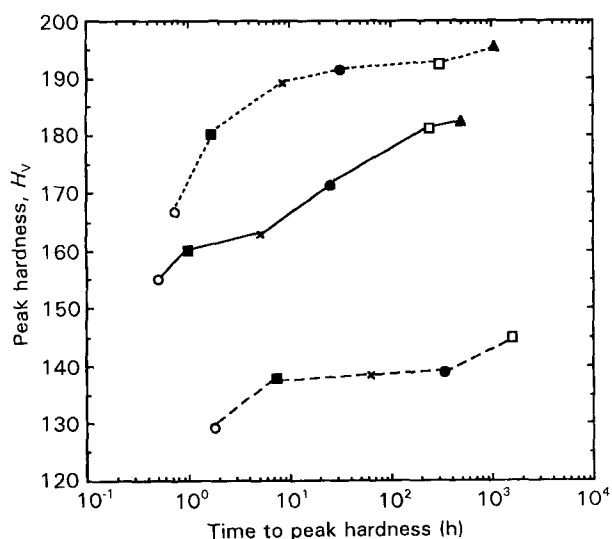


Figure 3 Variation in peak ageing condition with ageing temperature for (—) solution-treated alloy, (---) solution-treated MMC and (· · ·) stretched MMC. Ageing temperature (▲) 110°C, (□) 130°C, (●) 150°C, (X) 170°C, (■) 190°C, (○) 210°C.

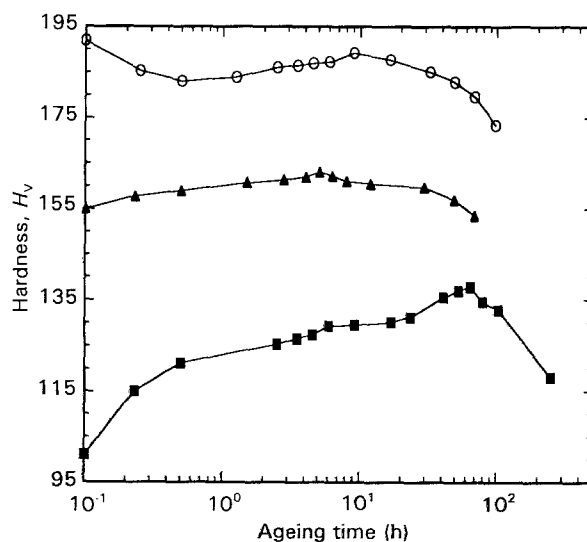


Figure 4 Ageing curves at 170°C for (■) unreinforced solution-treated alloy, (▲) solution-treated MMC and (○) stretched MMC.

The initial drop in hardness seen in all ageing curves of the stretched MMC (Fig. 4) has been attributed to dissolution of Guinier–Preston B (GPB) zones formed during natural ageing [23]. The stretched MMC also shows slightly longer times to peak hardness than the re-solution treated MMC (Figs 3 and 4). This is the opposite trend to the commonly observed behaviour in unreinforced Al alloys [19, 20] and has been attributed to an increased incubation period for  $S'$  formation [23] brought about by the extended natural ageing of this MMC and a resultant lack of available solute in solution.

#### 3.2. Activation energies for diffusion

Fig. 5 shows the Arrhenius plots for the three materials. The activation energy for diffusion in the unreinforced alloy is found to be 147 kJ mol<sup>-1</sup>. This is similar to that previously determined (158 kJ mol<sup>-1</sup>) for the peak aged condition in Al–Cu–Mg alloys [24].

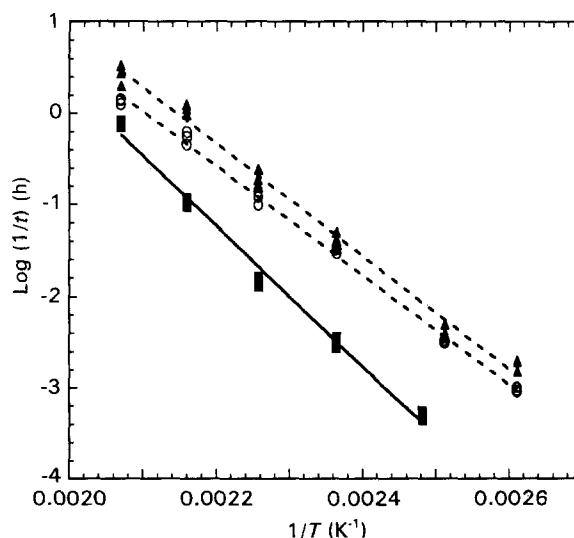


Figure 5 Arrhenius plots for (■) unreinforced solution-treated alloy, (▲) solution-treated MMC and (○) stretched MMC.

TABLE I Diffusion data for Al alloys

Type of diffusion	$Q$ (kJ mol <sup>-1</sup> )
Bulk diffusion-Al in Al	123-126
Bulk diffusion-Cu in Al	126-136
Bulk diffusion-Mg in Al	115-130
Bulk diffusion-Cu in Al/Cu	120
Bulk diffusion-Al + Cu in Al-Cu	122-130
Grain boundary diffusion-Al in Al	60-87
Grain boundary diffusion-Cu in Al	105
Grain boundary diffusion-Cu in Al-Cu	100
Grain boundary diffusion-Al + Cu in Al-Cu	84-98

A survey of the data for elemental diffusion in Al alloys is given in Table I [25-28]. This shows that the value of  $Q$  obtained for the unreinforced alloy is above the values for bulk diffusion, presumably due to the competitive diffusion of several solute elements in the unreinforced alloy, whereas the data in Table I were obtained in pure Al or simple binary systems.

The activation energy for diffusion is calculated to be 114 kJ mol<sup>-1</sup> in the stretched MMC and 118 kJ mol<sup>-1</sup> in the re-resolution treated MMC. These values are somewhere between the values for bulk diffusion and grain boundary diffusion in Table I. The stretched MMC might be expected to show a lower activation energy because of the increased density and homogenization of dislocations. Although this is the case, the similarity of the activation energies for the two MMCs suggests that stretching the MMC has only a minor effect on diffusion. This is to be expected since the effect of the dislocations produced during the stretch is likely to be small compared to the high dislocation density already induced by the thermal mismatch stresses.

The values of  $Q$  in the MMCs are approximately 21% lower than for the unreinforced alloy, suggesting that diffusion is easier in the MMCs. Unfortunately, there are few published data in this area with which to compare the current results. Nieh and Karlak [11], working on 6XXX matrix MMCs, found the same trend as in the current work with the activation energy for diffusion being 37% lower in the MMC than in the unreinforced alloy. Nieh and Karlak attributed the reduction in activation energy for diffusion in the MMC to enhanced diffusion of solute along dislocations to growing intermediate precipitates. This is likely to be the case in the current MMC, with additional diffusion along the SiC<sub>p</sub>-matrix interfaces also contributing. The MMC also has a larger grain boundary area than the unreinforced alloy, due to the smaller sub-grain size, and this is also likely to contribute to enhanced solute diffusion.

### 3.3. Differential scanning calorimetry

Fig. 6 shows representative scans for the three materials. Each scan consists of an exothermic trough at approximately 65 °C, an endothermic peak at 200-230 °C and an exothermic trough at approximately 260 °C. These have previously been attributed to GPB zone formation, GPB zone dissolution and S' formation

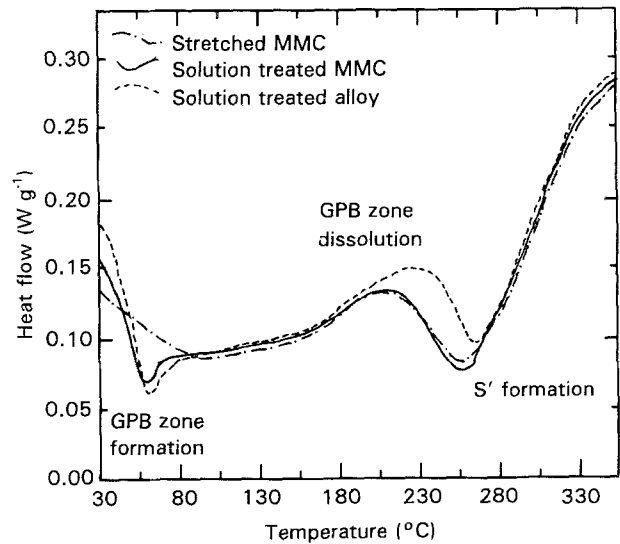


Figure 6 Representative DSC scans for (---) solution-treated alloy, (—) solution-treated MMC and (-·-) stretched MMC.

formation, respectively [1, 29, 30]. No GPB zone trough occurs in the stretched MMC, suggesting that it contains a high density of GPB zones, formed during natural ageing, with little further formation during the DSC scan. The trough corresponding to S' precipitation does occur in the stretched MMC, indicating that no appreciable quantity of S' has developed during natural ageing.

The onset temperatures, peak temperatures and peak enthalpies for the materials are given in Table II. The three DSC scans for each material gave consistent results, as indicated by the low values of standard deviation ( $\sigma_n$ ). Onset temperatures mark the point at which precipitate nucleation begins, whilst the peak temperature corresponds to the point of maximum enthalpy of formation. The area inside the DSC troughs is the total enthalpy of precipitate formation and gives an indication of the total volume of precipitate formed [31].

#### 3.3.1. GPB zone formation

The GPB zone peak enthalpy is 53% lower in the re-resolution treated MMC than in the unreinforced alloy. This phenomenon is commonly seen [1, 29, 30] and has been explained in terms of the free vacancy concentration. The high dislocation density in the MMCs in the as-quenched condition leads to the vacancy concentration being much lower than in the unreinforced alloy, because dislocations act as vacancy "sinks". Vacancies are required for the nucleation of GPB zones so fewer stable GPB zones are formed in the MMC [29, 32]. The fact that fewer GPB zones form in the MMC is confirmed in this and other work [29, 33] by the enthalpy of GPB zone dissolution being less in MMCs than in unreinforced alloys, as measured on DSC scans.

The onset and peak temperatures of GPB zone formation are reduced in the re-resolution treated MMC compared to the unreinforced alloy. This suggests that GPB zone nucleation requires a lower

TABLE II Data from DSC scans

Material	GPB onset temperature (°C)	GPB peak temperature (°C)	GPB peak enthalpy (J mol <sup>-1</sup> )	S' onset temperature (°C)	S' peak temperature (°C)	S' peak enthalpy (J mol <sup>-1</sup> )
Unreinforced Al alloy	51.8 $\sigma_n = 0.7$	67.3 $\sigma_n = 0.7$	9.3 $\sigma_n = 1.6$	252.5 $\sigma_n = 0.9$	264.7 $\sigma_n = 0.3$	5.4 $\sigma_n = 0.8$
Resolution treated MMC	44.4 $\sigma_n = 3.4$	64.5 $\sigma_n = 0.8$	5.5 $\sigma_n = 0.3$	219.2 $\sigma_n = 1.7$	255.5 $\sigma_n = 1.2$	24.4 $\sigma_n = 2.5$
Stretched MMC	—	—	0.0	217.3 $\sigma_n = 3.1$	255.8 $\sigma_n = 1.8$	20.7 $\sigma_n = 3.3$

driving force in the MMC. This appears to conflict with the “decreased vacancy content” idea which leads to the expectation that onset and peak temperatures of GPB zone formation would be higher in the MMC [32], as has occasionally been observed experimentally [29]. A significant number of studies, however, confirm the observed reduction in GPB zone onset and peak temperatures [1, 7, 30, 34]. The onset and peak temperatures have been also found to decrease as the reinforcement content increases [7, 34].

A mechanism to explain the apparently contradictory observations of enhanced GPB zone nucleation but decreased GPB volume in the MMC requires the existence of two types of location within the MMC, each with different precipitation capabilities. In a particulate MMC such regions would be (i) the high dislocation density, high strain zone around SiC<sub>p</sub> and (ii) the bulk matrix away from reinforcement. It is suggested that GPB zone formation then occurs by the following mechanism, which is consistent with the current DSC results and detailed microstructural investigations reported in the literature.

1. During quenching from the solution treatment temperature the SiC<sub>p</sub> cool more slowly than the matrix, since the particles have a lower thermal conductivity. This results in the matrix around SiC<sub>p</sub> (region (i)) being warmer than the bulk matrix (region (ii)). Diffusion of vacancies and solute atoms will occur to the higher solubility of the particle–matrix interfacial region, so that at the onset of ageing region (i) is vacancy and solute rich [34]. GPB zone formation will, therefore, be promoted in this region.

2. Around the SiC<sub>p</sub> (region (i)) the local stress field may also encourage GPB zone formation. Such an effect has been observed during artificial ageing of an Al–Cu alloy [35]. When a compressive stress was applied during ageing, GP zones formed preferentially on [100]<sub>z</sub> planes perpendicular to the applied stress. Similar behaviour has been observed for  $\theta'$  in an Al–Cu/SiC<sub>p</sub> MMC, where  $\theta'$  precipitation was enhanced in certain orientations with respect to the local thermal expansion mismatch stress [36]. The GPB zones in the present case are Cu-rich [37] and so have a negative misfit parameter. Since GPB zones are rod-shaped [38], their alignment with the local stress field so that their sides are perpendicular to any compressive stress could lead to a significant reduction in strain energy and hence promote GPB zone formation

in the SiC<sub>p</sub> interfacial region (region (i)). This could contribute to the reduced GPB zone onset temperature on DSC scans.

3. The high dislocation density in the interfacial region provides many sites for vacancy annihilation and as ageing progresses the vacancy density rapidly decreases. So after an initial period of easy GPB zone nucleation in region (i), nucleation and growth become increasingly difficult, and the total volume of GPB zones formed in the interfacial region is small.

4. The initial vacancy concentration in the bulk matrix (region (ii)) will be lower than in region (i), resulting in the initial GPB zone nucleation rate being lower in the bulk. The annihilation of vacancies during ageing will be slower in the bulk than in region (i), however, due to the lower local dislocation density. So after the initial period of rapid GPB zone nucleation in the interfacial region, GPB zone nucleation and growth will become energetically easier in the bulk matrix. Thus, during the complete ageing cycle, the total amount of GPB zones formed in the bulk may be greater than in the interfacial region, as has been observed using TEM on a 2XXX matrix MMC [36].

5. The total GPB zone density in the MMC matrix will, however, be lower than in the unreinforced alloy because of the overall increased vacancy annihilation at dislocations during ageing.

### 3.3.2. S' formation

The S' onset and peak temperatures are the same in both MMCs. Although the stretched MMC has a lower S' enthalpy, the standard deviation shows that this is not significant. These observations are unexpected since stretching has been shown to decrease the peak S' temperature and to increase the peak enthalpy in both 2XXX alloys and MMCs [21], because of the enhanced dislocation density. It has been noted, however, that the enhancement of S' formation in stretched MMC compared to unstretched material decreases as the reinforcement content increases [21], so that at additions of 20 wt % little difference is seen. This is presumably due to the strong effect of the thermal mismatch dislocations, which swamp any effect of the stretch. This is shown further by work on cold rolling of a 6XXX matrix MMC. At reinforcement levels of 15 vol %, reductions of up to 75% have minimal effect on the DSC traces of intermediate precipitates [39].

The S' peak occurs 9°C lower in the MMCs compared to the unreinforced alloy as is commonly noted [1, 30], suggesting that S' nucleation occurs more readily in the MMCs. S' nucleates heterogeneously on dislocations and will therefore benefit from an increase in dislocation density such as is found in the MMCs [32]. The surface of SiC<sub>p</sub> may also provide preferential nucleation sites for intermediate precipitates [40, 41]. The enthalpy of S' formation in the Al alloy is approximately 20% of that of the two MMCs. This suggests that not only is S' nucleation made easier in the MMCs but that S' growth is encouraged compared to the unreinforced alloy. TEM observation has shown a high concentration of S' near the matrix-particle interface, indicating the importance of dislocation density for S' formation [30, 32]. Several studies have seen a reduction in the peak enthalpy of S' formation in MMCs compared to the unreinforced alloy [1, 29, 30] which has been linked in one case to an apparent retardation of S' precipitation in the MMC [1]. This has been attributed to a higher intermetallic content in the MMC compared to the unreinforced alloy due to incomplete solutioning [1], resulting in much of the solute being unavailable for S' formation.

Image analysis was used to assess the intermetallic content of the current materials using photomicrographs of long-transverse sections polished and etched in Keller's reagent. The intermetallic contents were 8.8 vol % in the stretched MMC, 5.6 vol % in the resolution treated MMC and 6.3 vol % in the resolution treated alloy. The MMC values were corrected to account for the 17.9 vol % of SiC<sub>p</sub>. The similarity of these intermetallic contents, compared to the large differences seen by Hunt *et al.* [1], means that the precipitation behaviour is unlikely to be affected by the relative intermetallic content of the materials in the current study.

#### 4. Conclusions

1. Ageing is accelerated in the MMC compared to the unreinforced alloy. The trend for increased peak hardness and increased time to peak hardness as the ageing temperature is decreased is, however, unchanged.

2. Stretching of the MMC results in higher hardnesses at all stages of ageing.

3. Activation energies for diffusion are lower in the MMC than in the unreinforced alloy, due to enhanced diffusion along dislocations, SiC<sub>p</sub>-matrix interfaces and grain boundaries.

4. GPB zone nucleation is accelerated in the MMC, whilst growth is retarded.

5. S' nucleation and growth is much increased in the MMCs, compared to the unreinforced alloy, because of enhanced diffusion of solute and increased density of heterogeneous nucleation sites in the MMC.

#### Acknowledgements

The authors thank Professor C. J. Humphreys for the provision of research facilities. M.P. Thomas acknow-

ledges the financial support of British Aerospace (Commercial Aircraft) and the SERC.

#### References

1. E. HUNT, P. D. PITCHER and P. J. GREGSON, in "Advanced Aluminium and Magnesium Alloys," Amsterdam, June 20-22, 1990 edited by T. Khan and G. Effenberg, (ASM International, Pennsylvania, 1991) p. 687.
2. D. M. KNOWLES, PhD thesis, University of Cambridge (1991) p.26.
3. T. CHRISTMAN and S. SURESH, *Acta Metall.* **36** (1988) 1691.
4. J. P. COTTU, J. J. COUDERC, B. VIGUIER and L. BERNARD, *J. Mater. Sci.* **27** (1992) 3068.
5. S. KUMAI, J. HU, Y. HIGO and S. NUNOMURA, *Scripta Metall.* **27** (1992) 107.
6. K. H. OH, H. I. LEE, T. S. KIM and T. H. KIM, in "Fundamental Relationships Between Microstructure and Mechanical Properties of Metal Matrix Composites", edited by M. N. Gungor and P. K. Liaw, (TMS, Warrendale, Pennsylvania, 1990) p. 115.
7. I. DUTTA, S. M. ALLEN and J. L. HAFLEY, *Metall. Trans.* **22A** (1991) 2553.
8. T. CHRISTMAN and S. SURESH, *Mater. Sci. Eng.* **102A** (1988) 211.
9. N. WHANG, Z. WANG, G. C. WEATHERLY, in "Fabrication of Particulates Reinforced Metal Composites," edited by J. Masounave and F. G. Hamel. (ASM International, Materials Park, Ohio, 1990) p. 145.
10. K. K. CHAWLA, A. H. ESMAEILI, A. K. DATYE and A. VASUDEVAN, *Scripta Metall.* **25** (1991) 1315.
11. T. G. NIEH and R. F. KARLAK, *ibid.* **18** (1984) 25.
12. A. WANG and H. J. RACK, in "Metal and Ceramic matrix Composites: Processing, Modelling and Mechanical Behaviour," Anaheim, CA, 1990, edited by R. B. Bhagat, A. H. Clauer, P. Kumar and A. M. Ritter (Minerals, Metals and Materials Society, Warrendale, Pennsylvania, 1990) p. 487.
13. S. WEIMING, L. GEYANG and L. PENXING, in "Fabrication of Particulates Reinforced Metal Composites," edited by J. Masounave and F. G. Hamel (ASM International, Materials Park, Ohio, 1990) p. 167.
14. L. SALVO, M. SUÉRY and F. DECOMPS, *ibid.*, p. 139.
15. M. FERRY, P. R. MUNROE and A. CROSKY, *Scripta Metall.* **28** (1993) 1235.
16. M. FERRY, P. R. MUNROE, A. CROSKY and T. CHANDRA, in "Advanced Composites '93", Proceedings of International Conference on Advanced Composite Materials, Wollongong, Australia, 1993, edited by T. Chandra and A. K. Dhingra (Minerals, Metals and Materials Society, Materials Park, Pennsylvania, 1993) p. 1259.
17. M. P. THOMAS, D. M. KNOWLES and J. E. KING, in "Euromat '91", Proceedings of 2nd European Conference on Advanced Materials and Processes, Cambridge, UK, 1991, Vol. 2, edited by T. W. Clyne and P. J. Withers (Institute of Materials, London, 1992) p. 105.
18. D. A. PORTER and K. E. EASTERLING, "Phase Transformations in Metals and Alloys" (Van Nostrand Reinhold, Wokingham, 1988) p. 68.
19. W. S. JUNG and J. K. PARK, *Scripta Metall.* **26** (1992) 831.
20. D. BROEK and C. Q. BOWLES, *J. Inst. Met.* **99** (1971) 255.
21. J. M. PAPAIZIAN and P. N. ADLER, *Metall. Trans.* **21A** (1990) 401.
22. M. VOGELANG, R. J. ARSENAULT and R. M. FISHER, *ibid.* **17A** (1986) 379.
23. M. P. THOMAS and J. E. KING, *Mater. Sci. Tech.* **9** (1993) 742.
24. H. MARTINOD, C. RENON and J. CALVET, *Rev. Mét.* **63** (1966) 815.
25. M. B. CHAMBERLAIN and S. L. LEHOCZKY, *Thin Solid Films* **45** (1977) 189.
26. K. PRYZBYLOWICZ, in Proceedings of 2nd International Symposium "Reinstoffe in Wissenschaft," Dresden, 1965, edited by J. Kunze, B. Pegal, K. Schlaubitz and D. Schulze (Akademie Verlag, Berlin, 1967) p. 587.

27. E. A. BRANDES and G. B. BROOK (eds), "Smithells Metals Reference Book," 7th Edn. (Butterworth-Heinemann, Oxford, 1992) p. 13–17.
28. I. KAUR, W. GUST and L. KOZMA, "Handbook of Grain and Interphase Boundary Diffusion Data," Vol. 1 (Ziegler, Stuttgart, 1989) p. 118.
29. J. M. PAPAIZIAN, *Metall. Trans.* **19A** (1988) 2945.
30. J. S. LIN, P. X. LI and R. J. WU, *Scripta Metall.* **28** (1993) 281.
31. M. I. POPE and M. D. JUDD, "Differential Thermal Analysis." (Heyden, London, 1977) p. 30.
32. T. W. CLYNE and P. J. WITHERS, in "An Introduction to Metal Matrix Composites" (Cambridge University Press, Cambridge, 1993) p. 378.
33. T. S. KIM, T. H. KIM, K. H. OH and H. I. LEE, *J. Mater. Sci.* **27** (1992) 2599.
34. J. L. PETTY-GALIS and R. D. GOOLSBY, *ibid.* **24** (1989) 1439.
35. T. ETO, A. SATO and T. MORI, *Acta Metall.* **26** (1978) 499.
36. P. B. PRANGNELL and W. M. STOBBS, in "Metal Matrix Composites—Processing, Microstructure and Properties," edited by N. Hansen, D. Juul Jensen, T. Leffers, H. Lilholt, T. Lorentzen, A. S. Pedersen, O. B. Pedersen and B. Ralph (Risø National Laboratory, Roskilde, Denmark, 1991) p. 603.
37. J. M. SILCOCK, *J. Inst. Met.* **89** (1961) 203.
38. G. W. LORIMER, in "Precipitation Processes in Solids," Conference Proceedings, Niagara Falls, 1978, edited by K. C. Russel and H. I. Aaronson (Metallurgical Society of AIME, Warrendale, Pennsylvania, 1978) p.87.
39. H. L. LEE, W. H. LU and S. L. I. CHAN, *Scripta Metall.* **25** (1991) 2165.
40. S. R. NUTT and R. W. CARPENTER, *Mater. Sci. Eng.* **75** (1985) 169.
41. G. LIU, Z. ZHANG and J. K. SHANG, *Acta Metall.* **42** (1994) 271.

*Received 3 March  
and accepted 22 April 1994*